Towards Green Data Center Microgrids By Leveraging Data Center Loads in Providing Frequency Regulation

Wenbo Qia and Jie Lia,*

a. Department of Electrical and Computer Engineering, Clarkson University, Potsdam, 13699, NY, USA.

Abstract. In an electricity grid, imbalance between generation and load need be corrected within seconds so that frequency deviations will not threaten the stability and security. This is especially important for a low inertia microgrid operated in islanded mode, which is equipped with a limited number of synchronous generators in regulating frequency. To this end, for data center microgrid with limited on-site generators and increased green energy, when isolated from the utility grid, frequency deviation due to generation-load imbalance could be potentially corrected by conventional generating units as well as data center loads. Focusing on high PV penetrated data center microgrid operated in islanded mode, this paper explores effective control strategies for data center loads to participate in primary frequency response. By analyzing unique operational characteristics of traditional and PV generation units, uninterruptible power supply (UPS) units, and power consumption characteristics of IT components and cooling systems, the proposed load control strategy design effectively utilizes primary FR capabilities while not compromising data center quality of service (QoS) requirements. simulations via MATLAB/Simulink Numerical effectiveness of the proposed load control strategy in enhancing renewable energy penetration without compromising the system stability and security, providing a viable solution for future green data centers.

KEYWORDS. Data Center, microgrid, load frequency control, primary frequency control, demand response.

1. Introduction

The rapid growth in the needs for data processing, storage, and communication leads to a proliferation of data centers that consist of (tens of) thousands of servers. The operation of such data centers requires extensive electric energy consumption. According to the Lawrence Berkeley National Laboratory (LBNL) report [1], data centers in the U.S. consumed over 70 billion kWh of electricity in 2014. Currently, data centers consume up to 3 percent of the global electricity production, and produce 200 million metric tons of CO₂ emission annually [2]. Indeed, it is projected that by 2030, data centers in the U.S. could consume up to 20% of electricity production, emerging as a new "polluter" with significant environmental impacts. To this end, high electricity bills and serious environmental concerns have attracted a lot of research on data center energy efficiency [3]-[7]. Specifically, some previous researches recommended using microgrids to provide electricity supply for data centers, which integrate onsite renewables and energy storages to guarantee high power quality, reliability, and sustainability requirements [3]-[5].

Data center microgrids can operate in both grid-connected and islanded modes. When grid-connected, data center microgrids will receive frequency support from the main grid; On the other hand, when operated in islanded mode, data center microgrids must maintain the frequency and voltage stability by itself. To this end, if a high penetration of renewable generation, such as PV, is integrated into the data center microgrid, uncertain power supply, together with volatile data center workload, may induce severe real-time generation-load imbalance. This could potentially lead to excessive system frequency deviations, and threaten the stability and security of data center electricity supply system [8]. Therefore, proper frequency regulation strategies are required for the stable operation of data center microgrid with increased renewable generation integration [9].

When islanded, frequency deviation induced by load changes in a microgrid is usually corrected by adjusting power outputs of traditional generating units, which is referred to as primary frequency control [10]. However, considering that in future data center microgrids with an increased penetration of renewables to pursue "green data center" objectives, system inertia and frequency response capabilities are greatly reduced while it becomes more expensive and technically difficult to perform such primary frequency control. To this end, researches in [11]-[12] recommended the usage of energy storage systems (ESS) to achieve frequency regulation of microgrids. However, this comes with two issues: (i) Installing ESSs in a microgrid may not be economically efficient, and (ii) life span of ESSs could be severely compromised due to charging-discharging cycles to provide frequency regulation. Therefore, designing proper load control strategy to support frequency regulation in microgrid is receiving more attentions [13]-[15].

Indeed, electrical loads of a data center represent good frequency response capabilities through effective load control. Electric loads of a data center microgrid include into two major categories: IT equipment loads (e.g., storage devices as well as processing and computing server machines) that normally consume about 36% data center energy, and cooling system loads (e.g., fans, air handlers, chillers, etc.) that usually consume about 50% data center energy [16]. IT equipment is mainly used to process two types of data center workloads, including delay-sensitive and delay-tolerant tasks. To this end, flexibilities of the IT equipment in processing delay-tolerant tasks as well as the cooling system in maintaining specific temperature range could be leveraged to control power consumption of data center over different time periods, and in turn regulate frequency of the data center microgrid.

This paper explores effective design and implementation of load frequency control in a data center to support the microgrid

*. Corresponding author **Jie Li**. Tel.: +1-856-256-5345 Current E-mail address: lijie@rowan.edu, Department of Electrical and Computer Engineering, Rowan University, Glassboro, 08028, NJ, USA E-mail address: qiw@clarkson.edu (Wenbo Qi) Tel.: +1-315-262-5992 system primary frequency regulation with increased PV integration. Specifically, unique characteristics of data center's cooling and IT loads will be analyzed to quantify their primary frequency regulation capabilities while not compromising data center quality of service (QoS) requirements. In this paper, we first use MATLAB/Simulink to build a data center microgrid simulation platform, which simulates traditional diesel generation units, PV generations, uninterruptible power supply (UPS), and power consumption model of data center (IT components and cooling system) while considering characteristics of data center electrical loads. Second, we propose an electric load control strategy to support primary frequency regulation of data center microgrid in islanded mode, and verify its effectiveness in helping maintain system frequency in comparison with the situation that primary regulation is only provided on the generation side. Last, the impacts of communication and actuation latency of data center load controllers as well as the actual response time of data center electric loads to such control signals on the overall performance of frequency regulation is analyzed.

The rest of the paper is organized as follows. Section 2 introduces models of major components of a typical data center microgrid. Section 3 presents the detailed control strategy for data center electric loads participating in primary frequency regulation. Numerical studies are presented in Section 4. Conclusions and future work are drawn in Section 5.

2. Simulation of a Data Center Microgrid

A typical data center microgrid consists of traditional diesel generating units, renewable generations such as PV units, automatic transfer switch (ATS), switchgear, UPS, power distribution units (PDU), and data center electric loads (including both IT and cooling loads), as shown in Fig. 1.

2.1 Diesel Generating Unit

Two diesel generating units equipped with speed governor and excitation system are simulated. The diesel units are directly connected to the data center's main bus, which are designed to provide primary frequency and voltage support as grid-forming units in islanded mode.

Fig. 2 shows P-f and Q-V droop characteristics of the diesel units, because the diesel unit's active power output is predominately coupled with terminal frequency, while the reactive power output is mainly dependent on its terminal voltage magnitude. When the frequency f reduces from point f to point f to point f to increase. Similarly, when the voltage magnitude f decreases from point f to point

2.2 PV Generating Unit

Renewable PV unit is simulated in our data center microgrid. The equivalent circuit of a PV cell is shown in Fig. 3(a), which includes light-generated current source I_{ph} , a diode D, a shunt resistance R_{sh} , and a series resistance R_s . Fig. 3(b) illustrates the $I_{PV}-V_{PV}$ and $P_{PV}-V_{PV}$ characteristics of a PV array. We can see

that there is a maximum power point on the P_{PV} – V_{PV} curve. To this end, the maximum power point tracking (MPPT) module is usually equipped to extract the maximum available power from a PV array.

As shown in Fig. 4, a PV array is connected to the data center microgrid main bus through a boost converter and a controllable inverter. The boost converter is regulated by MPPT control, and the inverter is regulated by PQ (active power and reactive power) control. Since PV generation units are usually designed as grid-following units, the reference frequency f of a PV unit must be taken from the data center microgrid main bus by a Phase Lock Loop (PLL).

2.3 Uninterruptible Power Supply

UPS systems are a crucial part of a data center microgrid, especially for the occasions that critical equipment must be protected from any potential power quality issues and power supply outage is not tolerable. Online UPS (as shown in Fig.5) can provide the most protection from any potential power outage and quality problems, such as transients as well as voltage sags and swells. AC power flowing through the UPS is converted to DC power, some of which charges the battery while the rest is inverted back to AC power for the connected equipment. The double conversion process essentially prevents power events, such as power fluctuations, power outages, and power surges, from reaching the equipment, thus yielding a preferable protection level.

UPS systems are normally designed to provide short-term power supply to data center equipment when electric outage happens, so as to give data center enough time to activate onsite backup generators. The size of the UPS battery bank is determined by the required time duration of power supply for the data center, which typically varies from 2~3 min to 7~10 min [17]. In our data center model, the Lead-acid battery is considered which can provide 5-minute power supply to data center.

2.4 Data Center Load

Power consumption of a data center is mainly from its IT components and cooling system [18]. As shown in Fig. 6, the former contains router clusters, Hard Disk Drive (HDD) clusters, and server clusters, while the latter consists of fans, Computer Room Air Handler (CRAH), and chillers [19]-[20]. IT components in a data center are usually divided into exclusive groups for handling different IT services, including data processing, computing, and storage tasks. That is, each component could be specified to process a unique type of IT services. In this study, we consider that all devices processing a same type of services are operated homogeneously, i.e., at the same frequency and power level.

1) IT component power consumption

Three types of IT services that are widely provided by data centers across the world are considered, including processing, computing, and storage. These services are further classified into two categories based on their distinct characteristics: delay-sensitive tasks and delay-tolerant tasks. Delay-sensitive means that a task must be processed immediately without delay, while delay-tolerant tasks refer to batch jobs that can be

completed within relatively loose deadlines. In this paper, processing and storage services are considered as delay-sensitive tasks, and computing services are considered as delay-tolerant tasks [19].

- Storage service: Two data center component clusters, HDD clusters and router clusters, are mainly used to provide storage services, such as upload and download actions. In this paper, power consumptions of HDD clusters and router clusters are formulated as linear functions of the task rate as in (1).
- Processing service: A processing service involves server, HDD, and router component clusters. Power consumptions of the HDD and router clusters can be similarly simulated as in (1). Server clusters could be operated under a set of discrete CPU frequency levels, and a certain level will be selected depending on the upcoming workloads as well as the quality of service requirements. Equation (2) calculates the power consumption of a server cluster, which includes power consumption related to the idle status, the server frequency f, and utilization.
- Computing service: A computing service is simulated as a delay-tolerant task in this paper. This task only involves server clusters, and the power consumption is formulated as in (3). Some computing tasks have pre-specified total execution time, measured in terms of number of computing hours on a single cluster capability. That is, tasks assigned to the data center would be completed within specified delay-tolerant time periods. Equation (4) enforces all computing tasks will be completed.

$$P_{i,t} = \frac{\lambda_{i,t}}{\lambda_i^{\max}} \cdot P_i^{\max}, \quad i \in T^{DS}$$
 (1)

$$P_{i,t} = B_i \cdot I_{i,t} + A_i \cdot (f_{i,l,t})^3 \cdot \frac{\lambda_{i,t}}{\lambda_i^{\max}}, \quad i \in T^{DS}$$
 (2)

$$P_{i,t} = P_i^{\text{max}} \cdot I_{i,t}, \quad i \in T^{DT}$$
(3)

$$\sum_{t=1}^{NT} \sum_{i=1}^{Ncom} I_{i,t} = DTT$$

$$(4)$$

$$P_t^{IT} = \sum_{i=1}^{Ncluster} P_{i,t}$$
 (5)

Where i, l, and t are indices of IT clusters, CPU frequency levels, and time periods. Decision variables include power consumption of IT component cluster P(kW), server frequency f(GHz), commitment of a component cluster I. Parameters include number of cloud service per unit task arriving at an IT cluster λ , power coefficients of a server cluster A and $B(kW/GHz^3, kW)$, delay-tolerant task time requirement DTT (seconds), number of computing clusters Ncom, number of IT clusters Ncluster, total time periods NT (seconds), maximum power level of an IT cluster $P^{max}(kW)$, set of delay-sensitive tasks T^{DS} , set of delay-tolerant tasks T^{DT} , and maximum capacity of an IT component cluster $\lambda^{max}(tasks/s)$.

The total power consumption of all IT clusters is calculated as in (5).

2) Cooling system power consumption

Generally, the cooling system of a data center consists of fans, Computer Room Air Handlers (CRAHs), and water chiller. IT clusters are cooled with cold air at temperature T_{in} , which is drawn through the chassis by fans and expelled at temperature T_{out} . Hot air returns through a CRAH where heat is removed and cooled to the cold air. CRAHs exchange the removed heat with a chilled water loop with cold water at temperature T_{water} . Finally, the cold water loop temperature is maintained by a chiller and cooling tower, which expels data center heat out [20].

Since all the heat generated by data center servers must be removed by air cooling. The thermodynamics of cooling the IT clusters can be captured by equation (6) [20].

$$k \cdot C \cdot M_{i,t} \cdot T_{out} = P_{i,t} + k \cdot C \cdot M_{i,t} \cdot T_{in}, i \in \left\{ T^{DS}, T^{DT} \right\}$$
 (6)

Where $P_{i,t}$ is the rate of heat removal (W) and is equal to the power withdraw of the IT clusters to maintain stable temperatures, k is the containment index, $M_{i,t}$ is the mass flow rate of air through the IT cluster (kg/s), and C is the specific heat capacity of air (J/g-k).

• Fan: The required flow rate through an IT cluster is achieved by forced air provided by the fans in this cluster. Fan power varies cubically with respect to the flow rate of air pushed (or sucked) by the device. Since flow rate varies linearly with respect to fan speed, the power consumption of fans in an IT cluster is calculated via (7).

$$P_{i,t}^{F} = P_{i}^{F,\max} \cdot (M_{i,t} / M_{i}^{F,\max})^{3}, i \in \{T^{DS}, T^{DT}\}$$
 (7)

Where $P^{F,max}$ is the maximum power of fan (kW), $M^{F,max}$ is the maximum flow rate through an IT cluster (cubic foot/minute).

The total power of all fans in the system can be calculated by (8).

$$P_t^{F,tot} = \sum_{i=1}^{Ncluster} P_{i,t}^F$$
 (8)

• *CRAH*: The total heat removed by all CRAHs is equal to the aggregate power consumption of all IT clusters, as described in (9). In addition, the amount of heat removed by a CRAH from the air can be calculated via equation (10).

$$\sum_{j=1}^{Ncrah} Q_{j,t} = P_t^{IT} \tag{9}$$

$$Q_{i,t} = EkC_{M_iv_i}^{0.7}[k_{T_{out}} + (1-k)_{T_{in}} - T_{water}], j \in CRAH$$
 (10)

In (10), E is the heat transfer efficiency of the air, M_j the mass flow rate of the CRAH, and v_j represents the fractional fan speed of the CRAH (from 0 to 1) which is used to calculate power requirement to run the CRAH itself as in (11).

$$P_{j,t} = P_j^{idle} + P_j^{dyn} \cdot v_j^3, \ j \in CRAH$$
 (11)

In (11), P^{idle} is idle power draw of CRAH (kW), P^{dyn} is dynamic power drawn of CRAH which is equal to the CRAH's maximum power minus idle power, and v can be achieved by solving equations (9) and (10).

The total power consumption of all CRAHs in the system is given as in (12).

$$P_t^{CRAH,tot} = \sum_{j=1}^{Ncrah} P_{j,t}$$
 (12)

• Chiller: The chiller accounts for the majority of the overall cooling power consumption in most data centers. In our data center microgrid, we consider a chiller capable of removing 2MW of heat, with a peak power consumption of 1.2MW with respect to the maximum loading. The power model of chiller is a function of total data center utilization (kW) as shown in (13), which can be derived based on empirical regression curves [21]. U_t is total data center utilization.

$$P_t^{chiller} = 185.7 \cdot U_t^2 + 461.2 \cdot U_t + 538.7 \tag{13}$$

The total power consumption of the entire cooling system is calculated as in (14).

$$P_t^{cool} = P_t^{F,tot} + P_t^{CRAH,tot} + P_t^{chiller}$$
(14)

3. Data Center Load Control Strategy

In this paper, load control refers to the adjustment of a proportion of the data center cooling and/or IT loads according to the microgrid frequency deviation, which will be able to provide frequency regulation capabilities similar as generators. To this end, both the active power output of traditional generating units and power consumption of controllable cooling and IT loads will be regulated quickly to balance power supply and demand, so as to restore the system frequency. This process is implemented in the primary frequency control of a data center microgrid.

In a data center microgrid with proliferated PVs, a sudden decrease of PV generation can lead to frequency drop of microgrid and terminal voltage swells of IT equipment, while a rapid increase in PV generation can result in bus frequency ascent and terminal voltage sags of IT equipment. Since IT equipment in data centers is very sensitive to large variation of frequency and voltage of the power supply, poor power quality can affect the performance of IT servers and even lead to property damage [22][23]. In addition, serious voltage and frequency variations might lead to unstable microgrid operation. Thus, over or under frequency protection devices are usually equipped to shut down IT equipment and/or cooling system. However, it will affect the QoS of data center services and economic benefits. To this end, an effective load control strategy to mitigate frequency and voltage fluctuations is an alternative option, especially when considering the increased penetration of renewables in future green data centers.

Frequency is regulated based on the measurement of frequency deviation. The load controller will be triggered once the system frequency deviation exceeds a certain threshold and the frequency deviation time is larger than the actuation delay (latency) T_{Delay} . The actuation delay T_{Delay} consists of three parts: the computation time, the communication time, and the controller actuation time [14][24].

The data center cooling and IT loads can be changed instantaneously by ON/OFF command signals. In this paper, the primary control goal is to maintain the system frequency deviation within 0.5 Hz. When a frequency deviation against a disturbance exceeds the threshold, the load controller will be activated to regulate frequency by adjusting controllable loads (cooling and IT). The frequency, measured at the point of common coupling (PCC) of the data center microgrid, is the

input to the controller.

The procedure of the proposed load controller is shown in Fig. 7. When the system frequency is higher than the nominal value plus a threshold Δf_{th} , a proportion of responsive cooling and IT loads (which were originally off) will be activated. In this occasion, IT loads will have higher priority to be activated, because processing more IT loads could bring higher benefits to data center owner. On the other hand, when the system frequency is lower than the nominal value minus a threshold Δf_{th} , a proportion of responsive cooling loads (which were originally ON) will be turned OFF. In this case, cooling loads will have higher priority for the same reason.

The above procedure is adaptive according to various levels of frequency deviation thresholds and load regulation proportions, as shown in Tables I-VI. This setup is to be tuned based on system specifications, in order to effectively utilize available load regulation capabilities to mitigate frequency deviations. For instance, comparing Tables III-VI with Tables I-II, when the PV penetration is higher, PV power output uncertainty could be more significant and would induce larger frequency deviation. In turn, more load control capabilities are expected for frequency regulation. The impact of actuation delay (latency) T_{Delay} is considered, with switching ON/OFF of cooling load actuation delay as 80 ms/20 ms, and switching ON/OFF of IT Load actuation delay as 120 ms/20 ms [14][24].

4. Case Study

In order to evaluate effectiveness of the proposed load control strategy, numerical experiments via MATLAB/ Simulink are performed to simulate various operation statuses of a data center microgrid. This microgrid consists of two 2MW diesel generators, one PV generation, one cooling system, and ten IT clusters (including one storage cluster, two processing clusters, and seven computing clusters) with 0.2MW power consumption each. Each IT cluster is connected to the data center microgrid bus through UPS. The PUE for data center is set as 2. Parameters of cooling loads (including Fans, CRAH, and Chiller) are set according to [16].

The following three cases are studied in a 16-second time period to evaluate effectiveness of the proposed control approach for regulating frequency of the data center microgrid in islanded mode. In all cases, PV power outputs are calculated with respect to the temperature of solar panels as 25 °C.

Case 1: Microgrid with 0.5MW PV integration (12.5% penetration).

Case 2: Microgrid with 1MW PV integration (25% penetration):

- (2.1) Without load control
- (2.2) With load control.

Case 3: Microgrid with 4MW PV integration (100% penetration):

- (3.1) Without load control
- (3.2) With load control

Case 1: Microgrid with 0.5MW PV integration (12.5% penetration)

In this case, the irradiance of sunlight falls from 1000W/m2 at

7s to 0W/m2 at 7.25s and returns back to 1000W/m2 from 12s to 12.25s. This leads the power output of PV to drop from 0.5MW to 0MW, then returns to 0.5MW, as shown in Fig. 8.

Fig. 8 shows frequency, voltage magnitude, power outputs of PV and two diesel generators, as well as total power loads of data center for the entire 16 seconds. We can observe from Fig. 8 that, PV power output changes do not drive frequency out of the range [59.5Hz, 60.5Hz]. In addition, voltage magnitude varies between 375V and 390V, which is also within the minimum voltage 372.4V (i.e., 0.95*392V) and maximum voltage 411.6V (i.e., 1.05*392V) corresponding to the desired 392V level. Fig. 9 further shows phase-to-ground terminal voltage magnitudes of the three phases for the IT clusters. It shows that terminal voltages of IT clusters are not significantly affected by power output change of PV, which is kept close to the desired 170V. This study shows that when the PV penetration level is not high, the fluctuation of PV power output may not bring significant frequency issue or other power quality concerns to data center microgrid.

Case 2: Microgrid with 1MW PV integration (25% penetration)

(2.1) Primary frequency control without load controller

In this case, the irradiance of sunlight falls from 1000W/m^2 at 7s to 0W/m^2 at 7.25s, which leads to the drop of the power output of PV from 4MW to 0MW as shown in Fig. 10. Fig. 11 shows the irradiance of sunlight rises from 0W/m^2 at 12s to 1000W/m^2 at 12.25s, which raises the power output of PV from 0MW to 4MW.

Fig. 10 shows frequency and voltage magnitude of data center microgrid main bus, active power output of PV and DGs, as well as total power demand of data center. It illustrates that, as power output of PV decreases, frequency goes below 59.5Hz and the under-frequency protection system of data center microgrid disconnects all UPSs and cooling systems to protect the physical assets. Although disconnected UPSs can temporally maintain sustained power supply to IT equipment, this frequent (due to fluctuations of PV outputs) and unexpected discharging (not triggered by power outages) could significantly compromise lifetime of UPSs, which is not economic due to high cost of UPSs. Fig. 11 further shows the same set of profiles when PV power output increases from 0 to 1MW. This triggers the bus frequency higher than 60.5Hz, and over-frequency protection system of data center microgrid disconnects all UPSs and the cooling system. Moreover, the bus frequency cannot be stabilized after disconnecting those assets. Such a frequency surge could damage diesel generators and transformers.

(2.2) Primary frequency regulation with load controller

In this case, besides two DGs, data center cooling system loads also participate in the frequency regulation based on our proposed control strategy. The power output of PV drops from 1MW at 7s to 0MW at 7.25s, and returns to 1MW from 12s to 12.25s.

Fig. 12 shows frequency and voltage magnitude of data center microgrid main bus, active power output of PV and

DGs, as well as cooling system and total power demands. From Fig. 12 we can see that 0.4 MW cooling load is cut off around 7.25s to pull frequency back to above 59.5Hz. On the other hand, 0.4 MW cooling load is restored around 12.25s to maintain frequency under 60.5Hz. Thus, as load can be effectively controlled to provide frequency regulation, over or under frequency protection system is not activated. Figs.12-13 further illustrate that both bus voltage magnitude and terminal voltages of IT clusters are within the acceptable range.

Case 3: Microgrid with 4MW PV integration (100% penetration)

(3.1) Primary frequency control without load controller

In this case, the irradiance of sunlight falls from 1000W/m^2 at 7s to 0W/m^2 at 7.25s which drops the power output of PV from 4MW to 0MW as shown in Fig. 14. Fig. 15 shows that irradiance of sunlight rises from 0W/m^2 at 12s to 1000W/m^2 at 12.25s, which raises the power output of PV from 0MW to 4MW.

The frequency and voltage magnitude of data center microgrid bus, active power output of PV and DGs, and total power demand of data center during the period of periods 6-7.2 seconds and 11-12.2 seconds are shown in Figs. 14-15. Same as Case 2.1, the under/over frequency protection system disconnects all UPSs and the cooling system when the bus frequency goes below 59.5Hz/above 60.5 Hz due to the sudden decrease/increase in PV generation. In addition, the entire microgrid system becomes unstable, and frequency is unable to return to the nominal value.

(3.2) Primary frequency regulation with load controller

In this case, besides two DGs, data center loads (both cooling and IT loads) also participate in the primary frequency regulation according to the proposed control strategy. The power output of PV drops from 4MW at 7s to 0MW at 7.25s, and rises back to 4MW from 12s to 12.25s.

The frequency and voltage magnitude of data center microgrid bus, active power output of PV and DGs, and total power demand of data center are shown in Fig. 16. From Fig. 16 we can see, 2 MW cooling load is cut off and the tasks of six computing IT clusters are shifted out to recover frequency back to above 59.5Hz, when PV generation decreases from 4MW to 0. When PV generation increases from 0MW to 4 MW, the tasks of six computing IT clusters are shifted in, and 2MW cooling load is also restored to pull frequency under 60.5Hz. Figs.16-17 further illustrate that both bus voltage magnitude and terminal voltages of IT clusters are within the acceptable range.

5. Conclusions

This paper presents a data center microgrid simulation model via MATLAB/Simulink, including traditional diesel generation units, PV generation, UPS, and power consumption model of data center (including IT components and cooling system) with the consideration of characteristics of data center loads. A data center load control strategy is proposed to allow data center loads participating in the primary frequency regulation, and is

verified by the microgrid simulation model. Numerical studies indicate that when the PV penetration is low, the sudden change in PV power output may not compromise microgrid frequency, and consequently load participation in the frequency regulation may not be critical. However, when the PV penetration is high (i.e., over 25% in our studies), traditional generators are not able to maintain microgrid frequency within the required range, and frequency regulation provided by data center loads becomes critical. To this end, case studies clearly illustrate the importance of load control to provide frequency regulation in future green data centers with extremely high % PV penetration levels.

References

- Shehabi A., S. J. Smith, N. Horner, et al. "United States data center energy usage report," *Lawrence Berkeley National Laboratory*, Berkeley, California, LBNL-1005775, pp. 4 (2016).
- [2] Data Center Knowledge, 2014. [online]. Available: http://www.datacenterknowledge.com/archives/2014/12/17/undertaking-challenge-reduce-data-center-carbon-footprint/
- [3] Jie Li, and Wenbo Qi. "Towards optimal operation of internet data center microgrid," *IEEE Transactions on Smart Grid*, 9(2), pp. 971-979 (2018).
- [4] Yu L., Tao J., and Yulong Z. "Distributed Real-Time Energy Management in Data Center Microgrids," *IEEE Transactions on Smart Grid*, 9(4), pp. 3748-3762 (2018).
- [5] Aksanli B., Akyurek A.S. and Rosing T. "Minimizing the effects of data centers on microgrid stability," Green Computing Conference and Sustainable Computing Conference (IGSC), 2015 Sixth International, pp. 1-9 (2015).
- [6] T. J. Chainer, M. D. Schultz, P. R. Parida, et al. "Improving data center energy efficiency with advanced thermal management," *IEEE Trans. Compon., Packag., Manuf. Technol.*, 7(8), pp. 1228–1239 (2017).
- [7] Koch, B. and Slezak, D. "Less energy, more efficiency in server rooms and data centers." *Computer Science-Research and Development*, pp. 1-2 (2017).
- [8] Femia N., Petrone G., Spagnuolo, G., et al. "Optimization of perturb and observe maximum power point tracking method," *IEEE trans. Power Electron.*, 20(4), pp. 963-973 (2005).
- [9] T. Senjyu, M. Datta, A. Yona, et al. "A control method for small utility connected large pv system to reduce frequency deviation using a minimal-order observer," *IEEE Transactions on Energy Conversion*, 24(2), pp. 520–528 (2009).
- [10] H. Han, X.C. Hou, J. Yang, et al. "Review of power sharing control strategies for islanding operation of ac microgrids", *IEEE Trans. Smart Grid*, 7(1), pp. 200-215 (2016).
- [11] L. Che and M. Shahidehpour. "DC microgrids: Economic operation and enhancement of resilience by hierarchical control," *IEEE Trans. Smart Grid*, **5**(5), pp. 2517–2526 (2014).
- [12] Zhao, Z., Yang, P., Xu, Z., et al. "Control strategy of energy storage system for frequency support of autonomous microgrid." In *Electrical Machines and Systems (ICEMS)*, 2015 18th International Conference on, pp. 422-426 (2015).
- [13] A. Molina-García, F. Bouffard, D.S. Kirschen. "Decentralized Demand Side Contribution to Primary Frequency Control," *IEEE Trans. on Power Syst.*, 26(1), pp. 411–419 (2011).
- [14] S. Pourmousavi, and M. Nehrir. "Real-time central demand response for primary frequency regulation in microgrids," *IEEE Transactions on Smart Grid*, 3(4), pp. 1988-1996 (2012).
- [15] J. Medina, N. Muller, I. Roytelman. "Demand Response and Distribution Grid Operations: Opportunities and Challenges," *IEEE Trans. on Smart Grid*, 1(2), pp. 193–198 (2010).
- [16] M. Dayarathna, Y. Wen and R. Fan. "Data Center Energy Consumption Modeling: A Survey", *IEEE Communications Surveys & Tutorials*, 18(1) (2016).
- [17] ABB. "Review: Data Centers," (2013).
- [18] R. Sawyer. "Calculating total power requirements for data centers," White Paper, American Power Conversion (2004).
- [19] Z. Chen, L. Wu, and Z. Li. "Electric Demand Response Management for Distributed LargeScale Internet Data Centers," *IEEE Trans. on Smart Grid*, 5(2), pp. 651–661 (2014).

- [20] D. Meisner and T. F. Wenisch. "Does low-power design imply energy efficiency for data centers?" in *Proc. 17th IEEE/ACM ISLPED*, pp. 109– 114 (2011).
- [21] Pelley, S., Meisner, D., Wenisch, T. F., et al. "Understanding and abstracting total data center power," In Workshop on Energy Efficient Design (2009).
- [22] R. Sawyer. "Calculating total power requirements for data centers", White Paper, American Power Conversion (2004).
- [23] G. Zhabelova, A. Yavarian, V. Vyatkin. "Data center power dynamics within the settings of regional power grid", *Emerging Technologies & Factory Automation (ETFA) 2015 IEEE 20th Conference on*, pp. 1-5 (2015).
- [24] A. A. Bhattacharya, D. Culler, A. Kansal, et al. "The need for speed and stability in data center power capping," in *Sustainable Computing: Informatics and Systems*, 3(3), pp. 183–193 (2013).

Figures and Tables

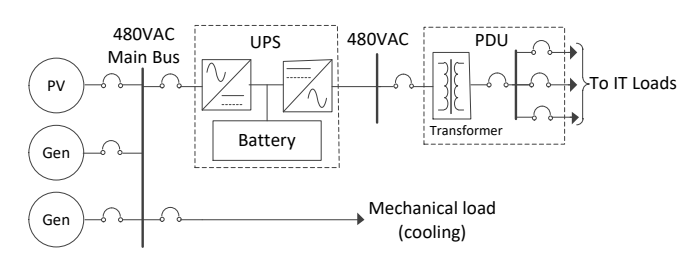


Fig. 1. A representative diagram of data center microgrid [15]

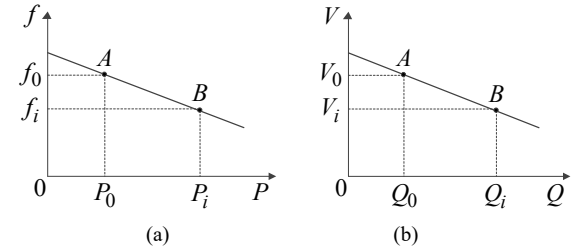


Fig. 2. Droop characteristics (a) P-f and (b) Q-V.

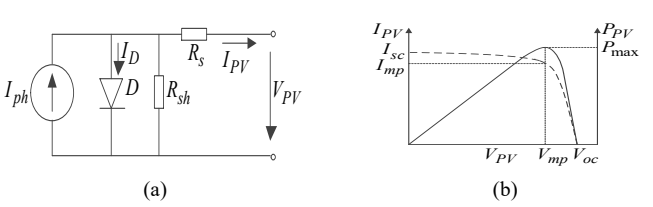


Fig. 3. PV cell (a) Equivalent circuit, (b) $I_{PV} - V_{PV}$ and $P_{PV} - V_{PV}$ characteristics.

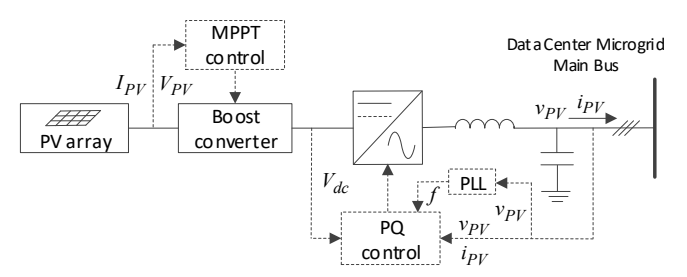


Fig. 4. Control structure of PV cell.

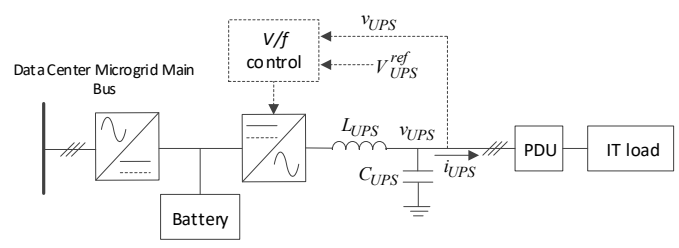


Fig. 5. Control structure of a UPS

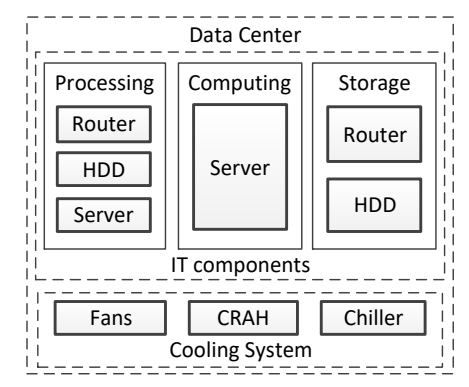


Fig. 6. Component clusters of a data center

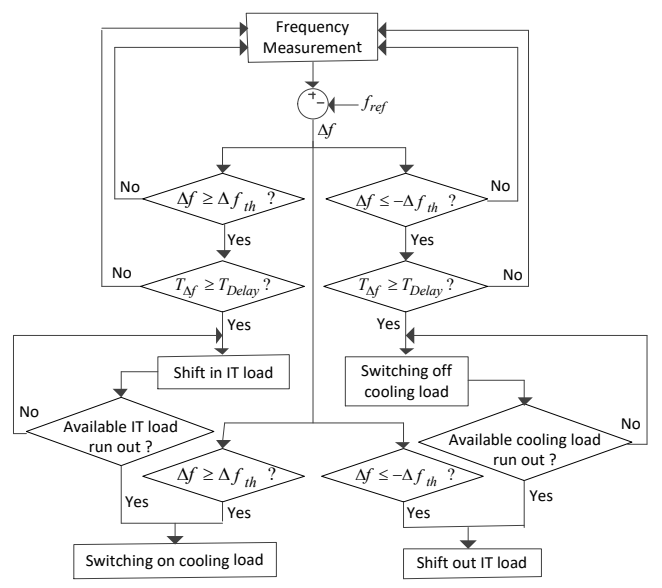
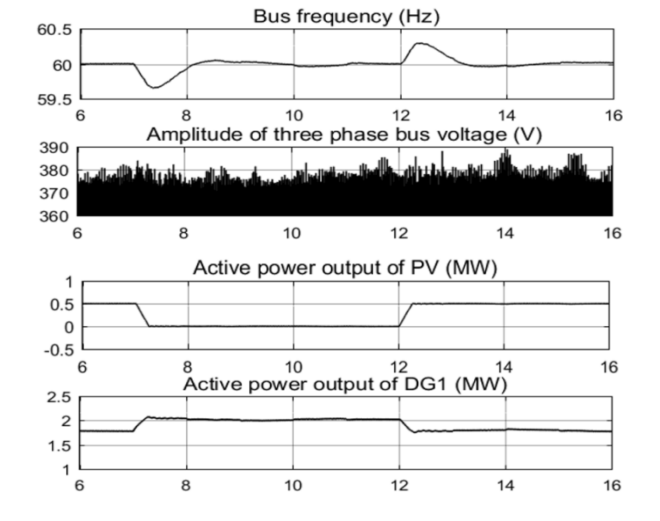


Fig. 7. Data center load control strategy



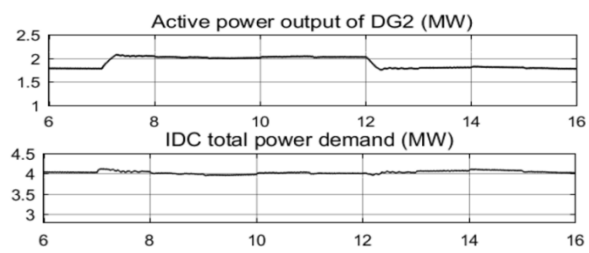


Fig. 8. Frequency and voltage magnitude of microgrid main bus, active power output of PV and DGs, and total power demand of data center in Case 1.

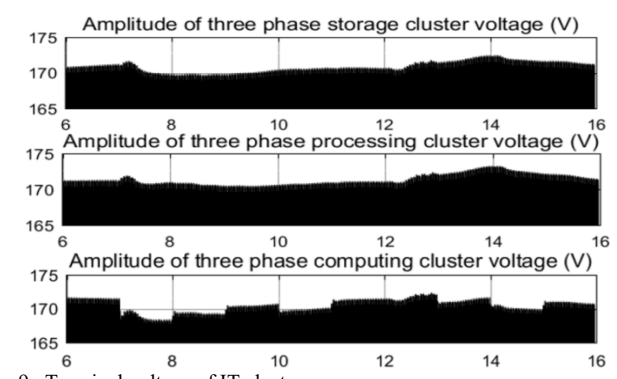


Fig. 9. Terminal voltage of IT clusters

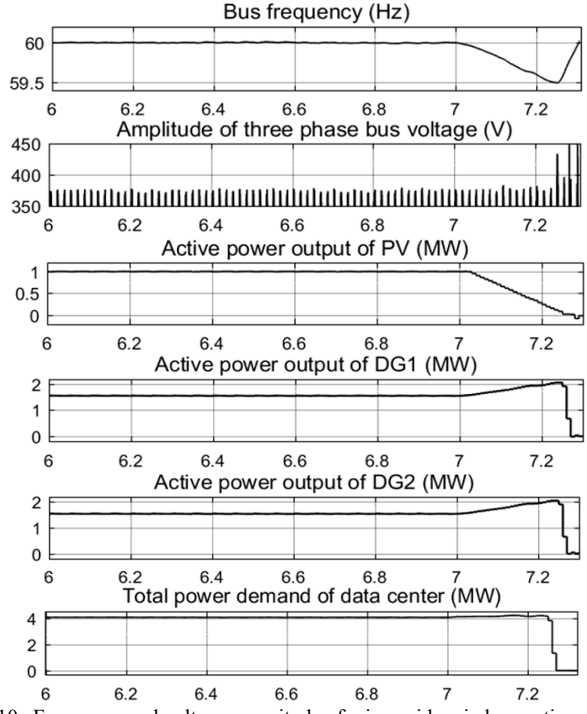
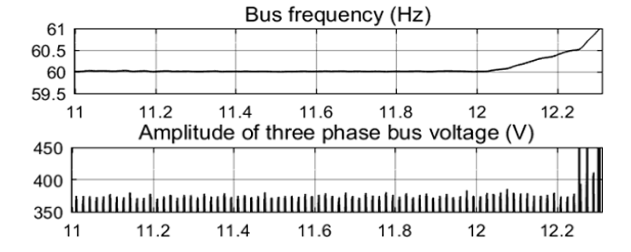


Fig. 10. Frequency and voltage magnitude of microgrid main bus, active power output of PV and DGs, and total power demand of data center in Case 2.1 from 6 second to 7.2 second.



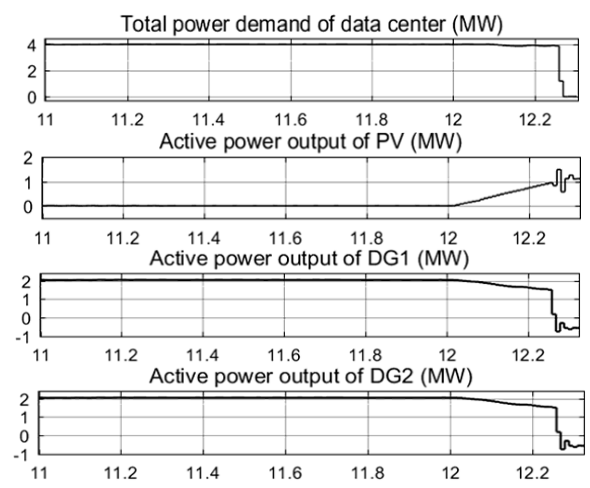


Fig. 11. Frequency and voltage magnitude of microgrid main bus, active power output of PV and DGs, and total power demand of data center in Case 2.1 from 11 second to 12.2 second.

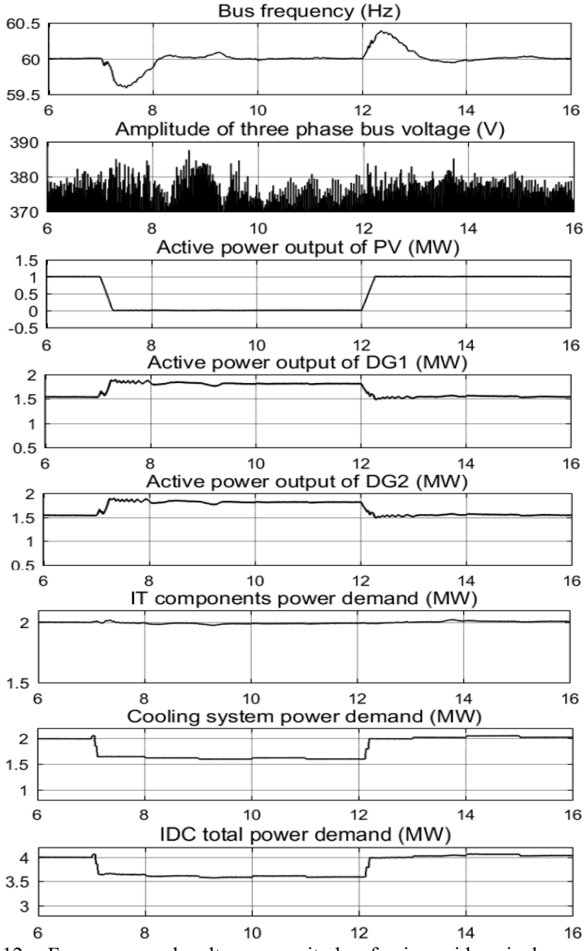
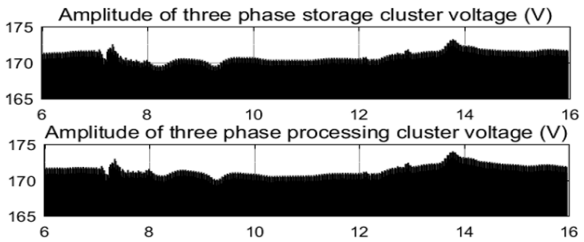


Fig. 12. Frequency and voltage magnitude of microgrid main bus, active power output of PV and DGs, as well as cooling system power demand and total power demand of data center in Case 2.2.



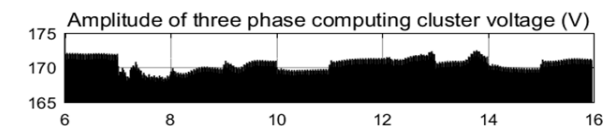


Fig. 13. Terminal voltage of IT clusters

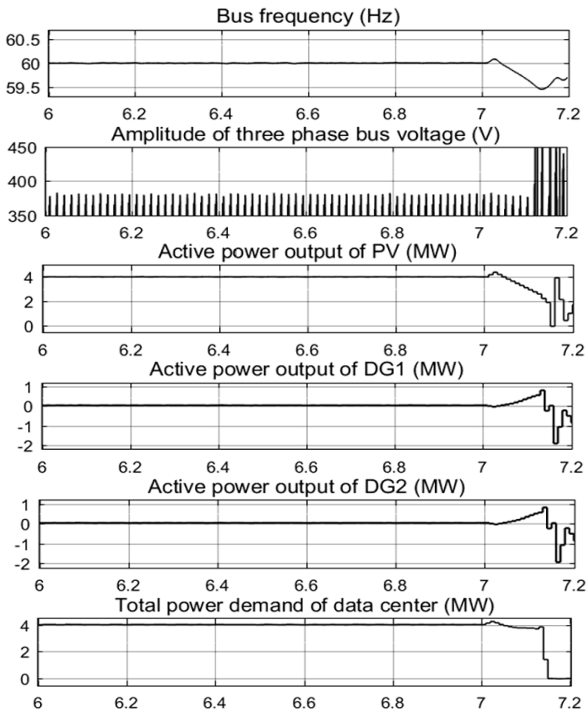


Fig. 14. Frequency and voltage magnitude of microgrid main bus, active power output of PV and DGs, and total power demand of data center in Case 3.1 from 6 second to 7.2 second.

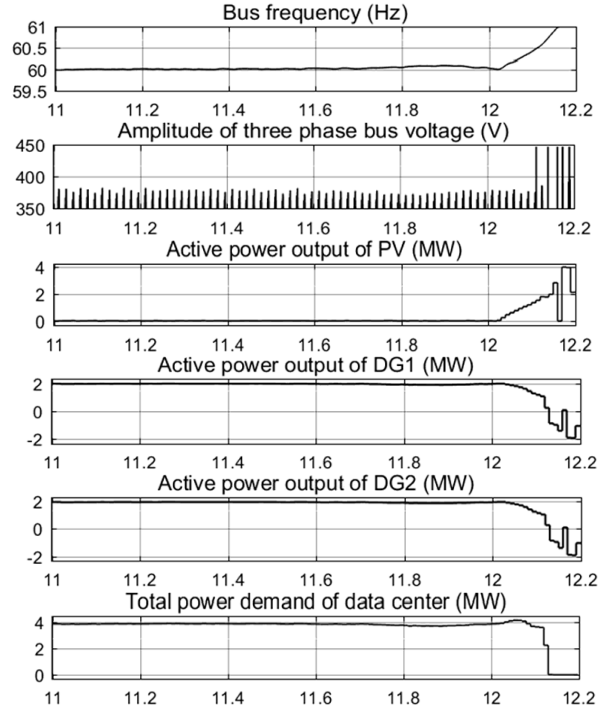


Fig. 15. Frequency and voltage magnitude of microgrid main bus, active power output of PV and DGs, and total power demand of data center in Case 3.1 from 11 second to 12.2 second

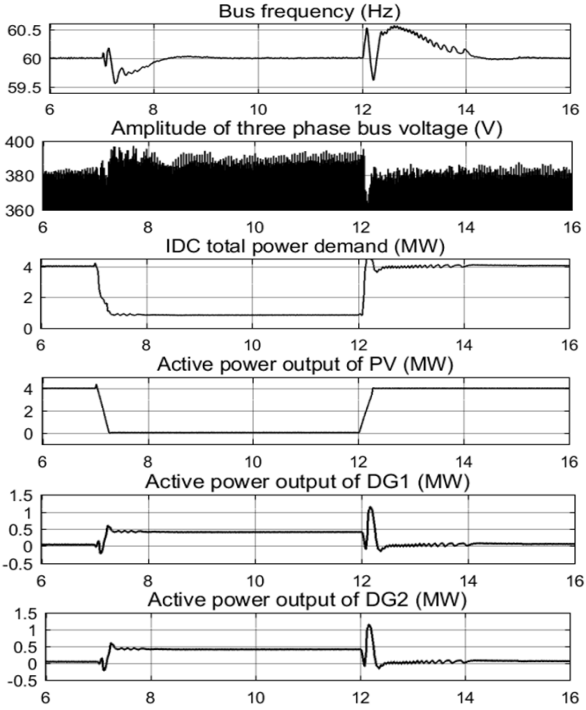


Fig. 16. Frequency and voltage magnitude of microgrid main bus, active power output of PV and DGs, and total power demand of data center in Case 3.2.

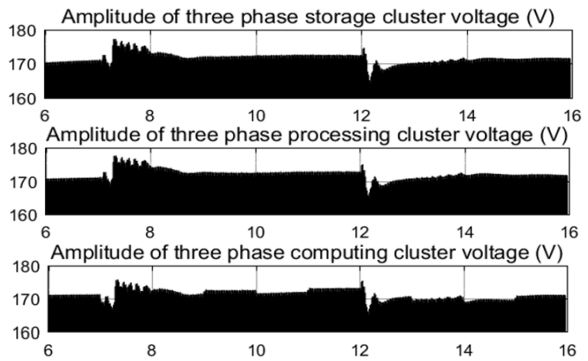


Fig. 17. Terminal voltage of IT clusters

TABLE I SHEDDING BEHAVIOR OF COOLING LOADS WITH 1MW PV

TABLET SHEDDING BEHAVIO			OK OF COOPERIO EOLED WITH THE W T
	Stages	Δf threshold	Cooling load regulation ratio
	1	-0.05Hz	10%
	2	-0.1Hz	20%

TABLE II ADDING BEHAVIOR OF IT LOADS WITH 1MW PV						
Stages	Δf threshold	IT load regulation ratio				
1	+0.05Hz	10%				
2	+0.1Hz	20%				

TABL	E III SHEDDING BEHA	VIOR OF COOLING LOADS WITH 4MW PV
Stages	Δf threshold	Cooling load regulation ratio
1	-0.02Hz	10%
2	-0.04Hz	20%
3	-0.06Hz	30%
4	-0.08Hz	40%
5	-0.1 Hz	50%
6	-0.12Hz	60%
7	-0.14Hz	70%
8	-0.16Hz	80%
9	-0.18Hz	90%
10	-0.2 Hz	100%

TARLEIV	SHEDDING BEHAVIO	R OF IT LOAD W	TH 4MW PV

Stages	Δf threshold	IT load regulation ratio
1	-0.22Hz	10%
2	-0.24Hz	20%
3	-0.26Hz	30%
4	-0.28Hz	40%
5	-0.3Hz	50%
6	-0.32Hz	60%

TABLE V ADDING BEHAVIOR OF IT LOADS WITH 4M	лW Р	4M	WITH 4	OADS	TL	OF I'	VIOR	BEHA	ADDING	TABLE V
---	------	----	--------	------	----	-------	------	-------------	--------	---------

Stages	Δf threshold	IT load regulation ratio
1	+0.02Hz	10%
2	+0.04Hz	20%
3	+0.06Hz	30%
4	+0.08Hz	40%
5	+0.1Hz	50%
6	+0.12Hz	60%

TABLE VI ADDING BEHAVIOR OF COOLING LOADS WITH 4MW PV

IADLI		OF COOLING LOADS WITH 4WIW I V
Stages	Δf threshold	Cooling load regulation ratio
1	+0.14Hz	10%
2	+0.16Hz	20%
3	+0.18Hz	30%
4	+0.2 Hz	40%
5	+0.22Hz	50%
6	+0.24Hz	60%
7	+0.26Hz	70%
8	+0.28Hz	80%
9	+0.3 Hz	90%
10	+0.32Hz	100%

Biographies

Wenbo Qi received his B.S. degree in Wind Energy and Power Engineering and Master of Electrical Engineering degree from North China Electric Power University, Beijing, China, in 2010 and 2013, respectively, and Ph.D. in EE from Clarkson University, NY, USA, in 2018. Presently, he is working as a Power System Developer in Open Systems International, Inc., Medina, Minnesota, USA. His research interests include green data center, demand response and power system modelling.

Jie Li received her B.S. degree in Electrical Engineering and M.S. degree in Systems Engineering from Xi'an Jiaotong University, China, in 2003 and 2006, respectively, and Ph.D. in EE from Illinois Institute of Technology, USA, in 2012. Presently, she is an Assistant Professor in the ECE Department at Rowan University, and before that, she is working at Clarkson University. Her research interests include green data center, demand response and electricity market bidding strategy.